2011 International Nuclear Atlantic Conference - INAC 2011
Belo Horizonte,MG, Brazil, October 24-28, 2011
ASSOCIAÇÃO BRASILEIRA DE ENERGIA NUCLEAR - ABEN
ISBN: **978-85-99141-04-5**

CHEMICAL AND MICROSTRUCTURAL CHARACTERIZATION OF RECYCLED ZIRCALOY

Luis G. Martinez[1], Luiz A. T. Pereira[1], Jesualdo L. Rossi[1], Hidetoshi Takiishi[1], Ivone M. Sato[2], Marcos A. Scapin[2], Marcos T. D. Orlando[3]

[1] Centro de Ciência e Tecnologia de Materiais - CCTM
Instituto de Pesquisas Energéticas e Nucleares, IPEN - CNEN/SP
Av. Prof. Lineu Prestes, 2242
05508-000 São Paulo, SP
lgallego@ipen.br, luiz.atp@uol.com.br, jelrossi@ipen.br, takiishi@ipen.br

[2] Centro de Química e Meio Ambiente - CQMA
Instituto de Pesquisas Energéticas e Nucleares, IPEN - CNEN/SP
Av. Professor Lineu Prestes, 2242
05508-000 São Paulo, SP
imsato@ipen.br, mascapin@ipen.br

[3] Departamento de Física - Laboratório de Altas Pressões - PRESSLAB
Universidade Federal do Espírito Santo - UFES
Av. Fernando Ferrari, 514 - Goiabeiras
29075-910 Vitória - ES
mtdorlando@gmail.com

ABSTRACT

PWR reactors employ as nuclear fuel UO_2 pellets with Zircaloy clad. Brazil is autonomous in the nuclear fuel cycle, from uranium mining to enrichment and nuclear fuel manufacture. However, the industrial production of nuclear zirconium alloys does not meet the demand, leading to importation of Zircaloy for fuel manufacturing. In the fabrication of fuel elements parts, machining chips of alloys are generated. As the Zircaloy chips cannot be discarded as ordinary metallic waste, the recycling of this material is strategic in economical and environmental aspects. In this work are described two methods that are being developed to recycle Zircaloy chips. The first method the Zircaloy machining chips are melted using an electric arc furnace to obtain small laboratory ingots. The second method uses powder metallurgy technique. By this later method, the Zircaloy chips are submitted to a hydriding process and the resulting material is milled in a high-energy ball mill. The powder is cold isostatically pressed and vacuum sintered. The elemental composition of the materials obtained using both methods is being determined using X-ray fluorescence techniques and compared to the specifications of nuclear grade Zircaloy and to the composition of the starting chips. The phase composition of the laboratory ingots was determined using X-ray diffraction. The ingots were vacuum annealed and the microstructures resulting from both processing methods before and after heat treatments were characterized using optical and scanning electron microscopy. The hardness of the materials was evaluated. A methodology of chemical analysis using X-ray fluorescence spectrometry, for composition certification, was established and tested. The results showed that recycled Zircaloy presented adequate microstructure for nuclear use. The good results of the powder metallurgy method suggest the possibility of producing small parts, like cladding cap-ends, using near net shape sintering.

1. INTRODUCTION

The nuclear fuel of PWR reactors is composed of uranium dioxide pellets - UO_2, assembled in metallic tubes called cladding. These tubes arranged in sets of 14x14 to 17x17 tubes form the fuel element. The retention of fission products is done, primarily, in the UO_2 ceramic pellets that accommodate part of the products of uranium fission. The second barrier is the cladding wall, which insulates the fuel from the water of the reactor primary circuit, which has moderator and coolant role. The cladding and structural components of the fuel elements are exposed to this water environment at high pressure and high temperature, besides high flux of energetic neutrons. This leads to extreme requirements of mechanical strength and corrosion behavior for these materials. Additionally, the nuclear cladding materials must present low absorption cross section for neutrons. The materials that best meet these requirements are known as Zircaloys. The Zircaloys are zirconium alloys that present excellent mechanical and corrosion properties and low absorption cross section for thermal neutrons. For low neutron absorption the zirconium has to be absent from hafnium, since this element has high absorption cross section for neutrons. The mechanical and corrosion properties are closely related to appropriate chemical compositions [1]. The zirconium alloys known as Zircaloy-2, Zircaloy-4 and Zirlo® are used in the manufacture of some reactor core parts, as claddings, coolant tubes tube guides and spacer grids [1-3]. Table 1 shows typical elemental compositions of Zircaloys [4, 5]. The advantage of Zircaloy-4 compared to Zircaloy-2 is its lower hydrogen absorption under water corrosion for PWR reactors [6]. Nuclear grade zirconium alloys are considered strategic materials and, therefore, beyond its high cost, are not freely commercialized. Thus, the production of zirconium alloys is a requirement for the autonomous domain of the process of nuclear power generation.

Table 1 - Typical composition of Zircaloy-2, Zircaloy-4 and Zirlo (mass %) [1, 4-6].

Element	**Sn** (%)	**Fe** (%)	**Cr** (%)	**Ni** (%)	**O** (%)	**Hf**	**Zr**	**Nb** (%)
Zircaloy-2	1.2-1.7	0.07-0.20	0.05-0.15	0.03-0.08	0.12	<100 ppm	bal.	-
Zircaloy-4	1.2-1.7	0.18-0.24	0.07-0.13	-	0.12	<100 ppm	bal.	-
Zirlo®	0-0.99	0.11	-	-	0.11	40 ppm	bal.	0.98

Zirlo® is a trade-mark from Westinghouse Electric Company. – Not specified.

Brazil has the technology for the production of nuclear fuel from uranium mining to manufacturing and assembly of fuel elements, including the isotopic enrichment process. However, the production of zirconium alloys is not carried out in the country at industrial scale and, therefore, the Zircaloy used in its nuclear power plants is imported.

In the fabrication of nuclear fuel elements parts, a great amount of Zircaloy residues like machining chips and scraps are generated and, as this material cannot be discarded as ordinary metallic waste, the recycling of this material presents a strategic role for the Brazilian Nuclear Policy due to economic and environmental aspects. In this work are described two methods that are being developed to recycle Zircaloy chips.

Compared to the production of new alloys the recycling of Zircaloy chips has advantages, once the starting material is already free of hafnium and has the specified composition. It is estimated that the economic savings in recovery of Zircaloy chips by electric arc furnaces is of US$ 78/kg [7]. In addition, the chips are generated in large quantities during the production of nuclear core parts, like the caps of the cladding tubes [8]. The caps of the tubes, also known as end-caps, shown schematically in Figure 1, are made by the machining of bars of Zircaloy. The machining chips generated by this process is contaminated by machining lubricants and surface oxides, must be long term stored in adequate conditions, once zirconium is pyrophoric and, also, nuclear grade Zircaloy is a controlled material. Thus, the recycling of this material gives, additionally, a destination to the stored material and may represent an economical advantage.

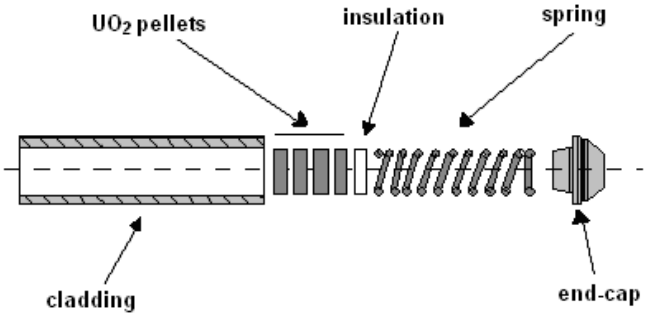

Figure 1 - Schematic drawing of the components of PWR rod fuel [8].

2. EXPERIMENTAL

2.1. Preparation of the material

The machining process of Zircaloy parts for fuel elements employs cutting oil, which impregnates the material. In order to remove the impurities, the chips were washed with a degreasing detergent and acid etched. It was, also, performed a manual magnetic separation of possible iron or steel particles. The washing procedure was repeated three times, 20 minutes each, using commercial neutral detergent and water in ultrasonic bath and then washed in deionized water. After the last washing, the material was dried with ethylic alcohol under a stream of heated air. The etching was done in two steps, firstly with HCl (50 HCl: 50 H_2O), followed by a second etch with HNO_3 (30 HNO_3 : 70 H_2O), 20 minutes each. The etched chips were washed using deionized water and dried using ethylic alcohol and heated air. The aspect of the cleaned material is shown in Figure 2 (a).

In order to accommodate the machining chips in the cavities of the furnace copper crucible and avoid dispersion of the electric arc, the material was compacted using two types of compaction dies; a circular (14 mm internal diameter) and a rectangular (13 x 32 mm). It was employed a hydraulic manual press and loads of 0.5 t (circular) and 1.5 t (rectangular). In Figure 2 (a) are shown examples of cleaned chips and two compacted briquettes and in Figure 2 (b) is show the rectangular die.

(a) (b)

Figure 2 - Zirconium machining chips after cleaning and compaction (a). Rectangular press die (b).

2.2. Electric arc furnace melting process

The melting of the machining chips was performed in a laboratory scale electric arc furnace with non-consumable electrode, under inert gas atmosphere (argon: 99.998% purity). The arc furnace consists of a tight hemispherical camera with water-cooled copper bottom, on which there are cavities to confine the melted metal. The non-consumable electrode (tungsten – 2 % ThO_2) is mounted on the extremity of a handle outside of the chamber. The vacuum system consists of a mechanical pump that allows pressure of 10^{-2} mm Hg inside the chamber. The system was evacuated and purged 3 times with argon and, finally, filled with argon at low pressure. The power supply for melting is an electric rectifier transformer. Before the fusion it was performed an acid pickling of the bottom to avoid material contamination [9]. For this purpose it was used an aqueous solution of HNO_3 20% followed by neutralization with deionized water and a final cleaning with acetone. In Figure 3 details of the arc furnace are presented: on left, the closed chamber and on right, the opened chamber, where it can be observed the cavities on the bottom. The operating conditions during the fusion were: current: 150 A; argon atmosphere pressure: 516 mm Hg.

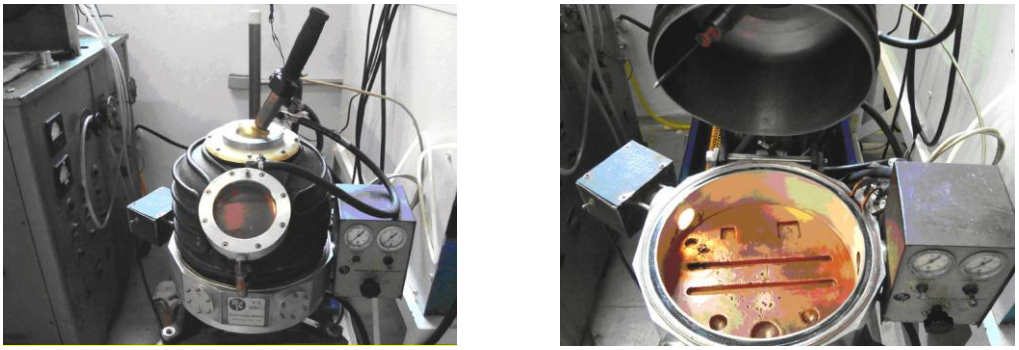

(a) (b)

Figure 3 - Images of the arc furnace: (a) with the chamber closed and (b) the opened chamber, showing details of the cavities on the bottom.

Four briquettes of compacted machining chips were placed inside a 10 mm width cavity to be melted altogether, resulting in a bar of 55 mm x 10 mm, as shown in Figure 4. This bar was used for the characterization studies.

Figure 4 - Photograph of the cast zirconium alloy bar.

Samples of both extremities of the bar were cut for microstructural characterization, chemical composition, hardness and X-ray diffraction. The microstructural analyses were performed in the cross section. The preparation consists of metallographic mounting on cold polyester resin followed by grinding with SiC sandpaper (200, 320 and 600 mesh) and electrolytic polishing (electrolytic polishing parameters: 3.5 V; 0.2 A; 30 sec; 1:10 electrolyte solution of 70% perchloric acid and glacial acetic acid).

2.3. Heat treatments

Three samples were submitted to two heat treatments at 800° C for 0.5 h and 1 h (samples 1A, 2A and 3A) and at 900° C for 0.5 h (samples 1D, 2D and 3D) to establish heat treatment time and temperature. The heat treatments were done in a resistive tubular furnace under vacuum (10^{-5} mbar).

The influence of heat treatments on the microstructure was studied using metallography and Brinell hardness measurements. The samples were cut using a precision saw, into two parts. One part was subjected to heat treatment and the other was used to compare the results before and after heat treatment. The heat treatments were performed in order to obtain a homogeneous microstructure and lower down the hardness, relatively to the as cast material, aiming subsequent mechanical work, like rolling.

2.4. Powder metallurgy process

Zirconium is one of the most suitable metals for powder metallurgy. Zirconium powder can be compacted and sintered close to its theoretical density. The sintered Zr is ductile and can be rolled, drawn and extruded. It is known [9] that hydrogen must be absorbed up to, at least, 50 % (atomic %) in zirconium, making the material brittle and adequate for its comminution. According to reaction kinetics studies of Zr and H_2, the significant absorption of hydrogen by

zirconium occurs from 235° C and has a maximum between 300° C and 375° C. After grinding, the material can be dehydrated during the sintering process under vacuum. The complete removal of hydrogen occurs at low pressure (10^{-5} mbar) and temperatures above 800° C [10].

The hydriding was carried out in a system composed by a stainless steel retort and a resistive tubular furnace. A circular compacted sample was placed in an alumina crucible and placed in the retort connected to an H_2 line and to the high vacuum system. Initially the system was evacuated to 0.3 mbar, purged with H_2 and then heated to 500° C. After temperature stabilization H_2 was injected for 5 minutes and then the retort was placed outside the furnace to be cooled at air. The hydride material was ground preliminary in an agate mortar and then in a high-energy planetary ball mill (zirconia balls diameter = 5 mm; proportion of powder 1 g: 10 g balls) with cyclohexane and grinded at 200 rpm for 30 min. The milled powder was dried under vacuum for 45 min and isostatically pressed at 200 MPa in a rubber mold (12 mm internal diameter). Part of the powder was reserved for determination of particle size distribution and X-ray diffraction measurements.

The sintering was carried out in a tubular resistive furnace under vacuum. The treatment started at room temperature until reaching a vacuum of 7 x 10^{-5} mbar, when the heating started at the rate of 8° C/min up to 1070º C. After 2 h at this temperature the pressure was stabilized at 4.8 x 10^{-6} mbar and the hydrogen was removed. The sintering was carried out at 1070° C for 20 h. The systems employed for hydriding and sintering are shown in Figure 5.

After sintering the sample was weighed and measured for determination of its apparent density, which was compared to the theoretical density of Zircaloy-4 (6.6 g cm^{-3}).

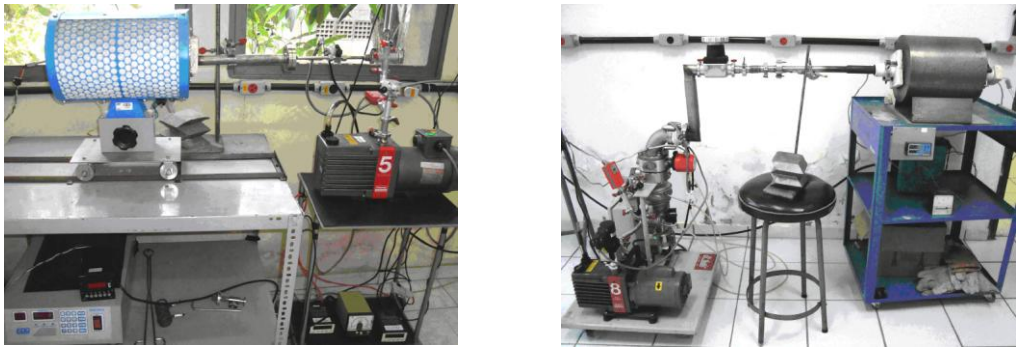

(a) (b)

Figure 5 - Hydriding system (a) and vacuum sintering system (b).

2.5. Characterization

The hardness was measured using a hardness tester with 1/16" diameter steel ball tip and a 100 kg load, using the Brinell hardness scale. Measurements were made in three regions along the flat section of the samples, maintaining a standard distance between them. The X-ray diffraction measurements were performed in a Rigaku diffractometer (model Ultima-IV) using Cu-K_α radiation.

The elemental composition of the samples was determined using X-Ray Fluorescence Spectrometry (XRFS), using a Shimadzu EDXRF spectrometer (model 720) and a Rigaku WDXRF spectrometer (model RIX 3000). The determination of elements Sn, Fe, Cr, Ni and Hf was performed using the fundamental parameters method and the sensitivity curve was obtained using standard and certified materials. The methodologies for sample preparation and data analysis were described elsewhere by Sato et al [8].

3. RESULTS AND DISCUSSION

3.1. Chemical analysis

The contents of Zr, Sn, Fe, Cr, Ni, Cu and Hf were determined using X-Ray Fluorescence Spectrometry (XRFS) and Zr was determined by mass difference. In Table 2 are presented, as example, the results for chemical composition of previous samples, obtained using electric arc melt before the magnetic separation and acid chemical etching. Although these previous samples presented contamination by steel, the study [8, 15] was developed in order to establish and evaluate the methodology for chemical analysis. The XRFS results for the samples presented in this work are not yet concluded and will be presented in a future work.

Table 2 – X-ray fluorescence analysis (mass %) of previous samples (LQ and TR) where it was found contamination by steel in comparison to specified compositions for Zircaloy-2 and Zircaloy-4 [8, 15].

Element	Sample LQ	Sample TR	Zircaloy-2	Zircaloy-4
Zr (%)	97.53	97.79	bal.	bal.
Sn (%)	1.74±0.35	1.60±0.30	1.2-1.7	1.2-1.7
Fe (%)	0.283±0.06	0.292±0.06	0.07-0.20	0.18-0.24
Cr (%)	0.240±0.06	0.157±0.04	0.05-0.15	0.07-0.13
Ni (%)	0.061±0.02	0.052±0.02	0.03-0.08	-
Hf ($\mu g\ g^{-1}$)	94±28	59±18	<100	<100

- Does not contain.

3.2. Microstructural analysis

The microstructural analysis of different sections of the melted bar showed that the homogeneity of the microstructure was not complete. The region in contact with the copper

bottom, where the cooling rate is high presents different microstructures compared to other sections, as show in Figures 6 and 7.

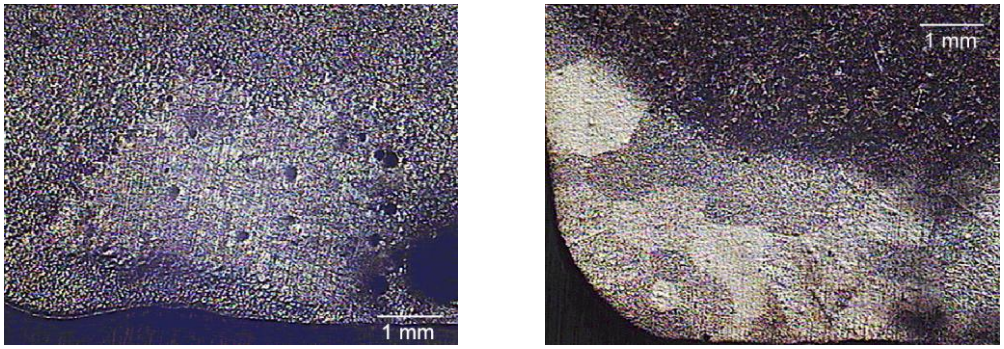

(a) (b)

Figure 6 - Optical macrographs of the samples: (a) bottom side of the melted bar (sample I2) and (b) top side of the melted bar (sample F2).

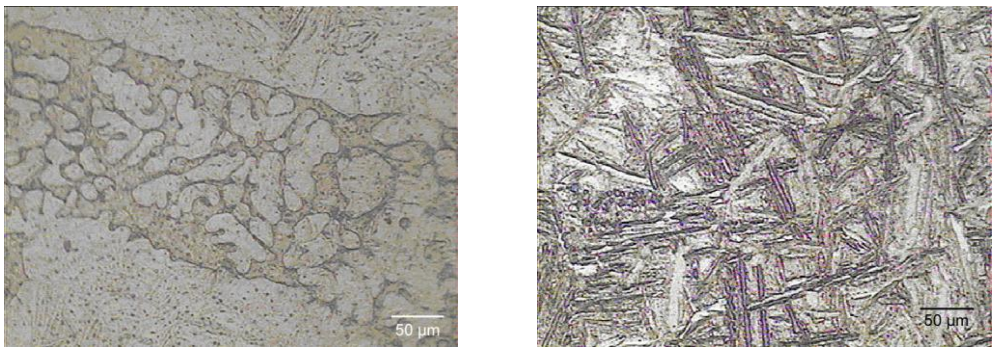

(a) (b)

Figure 7 - Optical micrographs of the samples: (a) bottom side of the melted bar (sample I2) and (b) top side of the melted bar (sample F2).

In Figures 8, 9 and 10 are shown the microstructures obtained before and after heat treatment.

(a) (b)

Figure 8 - Optical micrographs of the samples before and after heat treatment at 800 °C for 0.5 h: (a) before (sample 1A) and (b) after (sample 1D).

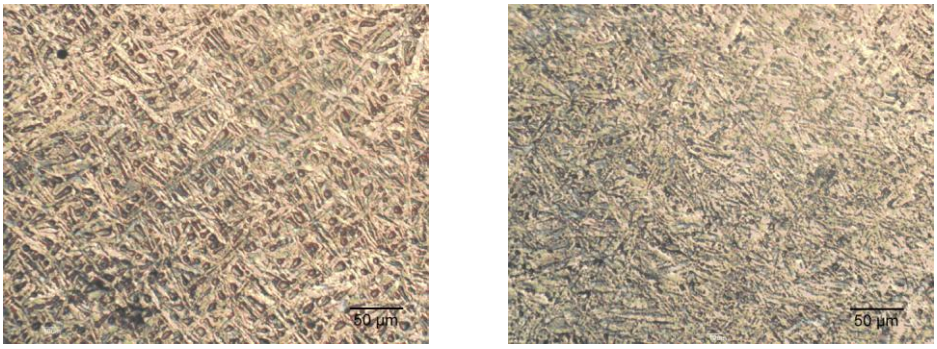

(a) (b)

Figure 9 - Optical micrographs of the samples before and after heat treatment at 800 °C for 1.0 h: (a) before (sample 2A) and (b) after (sample 2D).

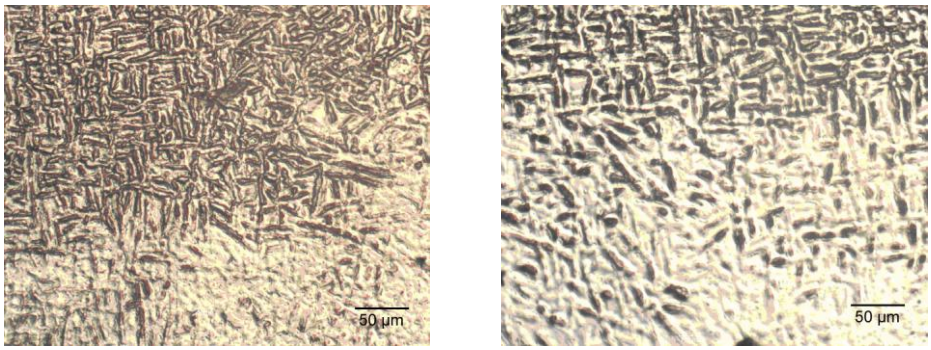

(a) (b)

Figure 10 - Optical micrographs of samples subjected to heat treatment at 900 °C for 0.5 h: (a) before (sample 3A) and (b) after (sample 3D).

According to the Zr-Sn binary diagram [9], on heating, pure zirconium undergoes an allotropic phase transformation from (α) hexagonal compact structure to (ß) BCC structure at 862° C. According to other work [11], the as cast microstructure of pure zirconium (basic composition of Zircaloy) is characterized by a *Widmanstätten* or a basketweave type microstructure. This is, probably, due to the existence of a high number of sites suitable for nucleation of plates, where the plates nucleated from phase ß grow toward the interior of the grains with preferred direction of growth [12]. According to the ASM and others [12, 13], the microstructure of cast samples is characterized by needles or platelets of martensite (α'). On slow cooling the α-phase nucleates on grain boundaries of ß-phase, forming an interlaced structure known as *Widmanstätten* type (or basketweave). When increasing the cooling rate the formation of a needle-shaped microstructure takes place, similarly to the typical martensitic microstructure of steels in appearance and mode of formation. In the literature [9] it is found that, in low-carbon steel, this structure is formed by strips or plates, which consist of several subunits of needles.

In Figure 11, are shown the microstructures of sintered Zircaloy-4 in three distinct regions, where can be observed a microstructure composed of rounded grains (a), the presence of needles (b) and the presence of pores (c) due to sintering. For improve the material quality, it is yet necessary to establish and optimize the parameters of sintering aiming to improve the

densification of the material. However, it can be pointed out that the microstructure of the sintered material is more homogeneous than the microstructure of the melted one.

(a) (b) (c)

Figure 11 - Optical micrographs from regions of the sintered sample at different magnification.

3.3. Hardness measurements

In Table 3 are shown the results of Brinell hardness for the melted samples. The hardness measured values are very close indicating that the heat treatment did not cause α to ß phase transformation in the melted material, as evidenced by similar microstructures before and after treatment.

Table 3 – Brinell hardness measured values for the melted Zircaloy samples.

Sample	**I2**	**F2**	**1A**	**1D**	**2A**	**2D**	**3A**	**3D**
Hardness (HB)	110	102	98	100	98	97	97	94

A-before and D-after heat treatment.

It can be pointed out that the microstructures before and after heat treatment are similar and the hardness of the material was slightly affected, as shown in Table 3.

3.4. Particle size and apparent density

The determination of particle size for Zircaloy-4 hydride powder by LASER scattering presented an average particle diameter of 5.06 µm. The sintered material presented an apparent density of 6.4 g cm^{-3}, which corresponds to 95% of the theoretical density of the metal [9], due to pores in the microstructure, as can be seen in Figure 11 (c).

3.5. X-ray diffraction

In Figure 12 are presented the diffractograms with full profile refinements (red line) of X-ray diffraction data (black cross) of melted (a), sintered (b) and hydrided (c) Zircaloy.

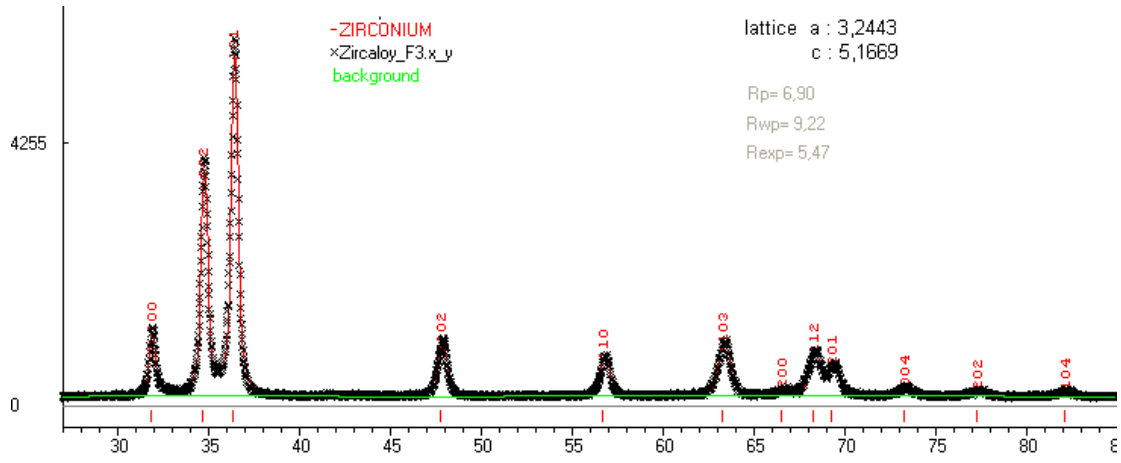

(a)

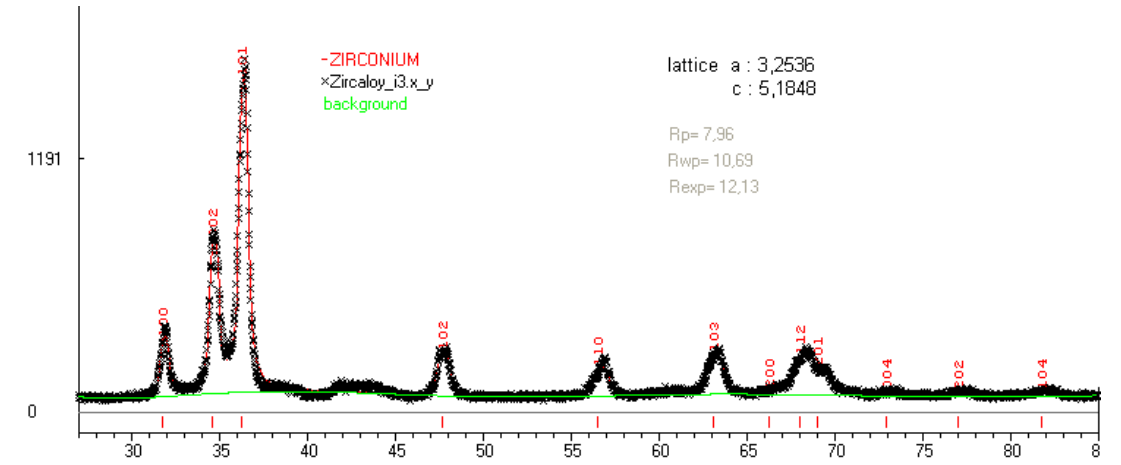

(b)

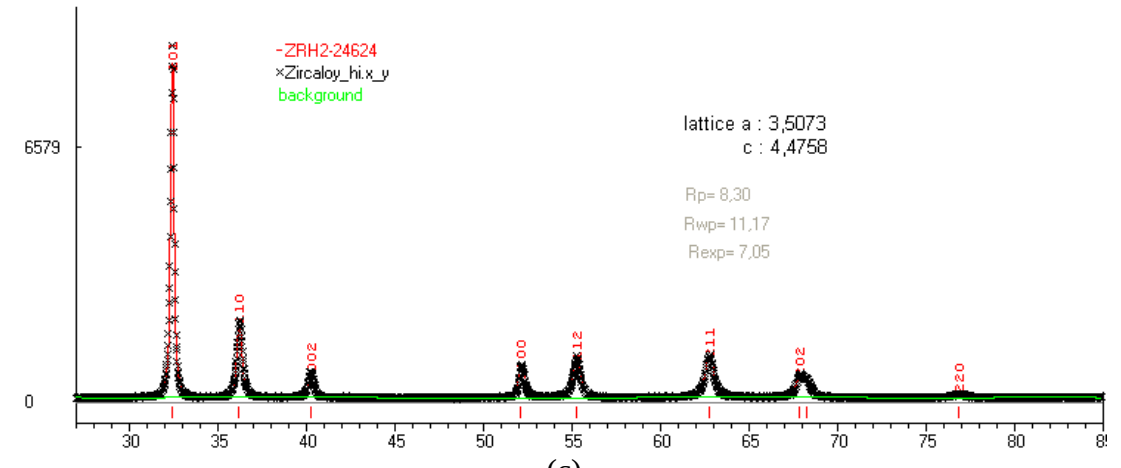

(c)

Figure 12 – Diffractograms and full profile refinements of X-ray diffraction data for samples: (a) Zircaloy obtained using arc melting; (b) Zircaloy obtained by sintering; (c) Zircaloy hydride powder.

Both the melted and the sintered Zircaloy presented hexagonal α-zirconium structure (Powder Diffraction File card number: 89-4892; Space Group P63/mmc) whit small difference in the cell parameters, as shown in Table 4. The sintered sample presented, also, a quantity of non-stoichiometric zirconium oxide (not refined) as can be seen in the diffractogram, between 38° and 46°. The hydrided Zircaloy was identified as tetragonal ZrH_2 (Powder Diffraction File card number: 17-314; Space Group I4/mmm) with cell parameters values presented in Table 4.

Table 4 – Results for Full Profile Refinements of X-ray diffraction data for melted, sintered and hydride Zircalloy

Sample	SG	Cell param. *a* (Å)	Cell param. *c* (Å)	PDF nº
Zry-melted	P63/mmc	3.2443	5.1669	89-4892
Zry-sintered	P63/mmc	3.2536	5.1848	89-4892
Zry-hydride	I4/mmm	3.5073	4.4758	17-314

4. CONCLUSIONS

It was demonstrated the effectiveness of the electric arc melting and powder metallurgy processes for recycling of Zircaloy machining chips.

It was established and evaluated a methodology for the determination of the chemical composition of recycled Zircaloy by X-Ray Fluorescence Spectrometry.

It was observed the necessity of avoiding contamination of Zircaloy chips with other material scraps or remove this contamination in order to obtain the specified composition in the recycled material.

The X-ray diffraction analysis shows that both, the melted and the sintered Zircaloy, presented α (hexagonal) zirconium structure.

The carried out heat treatments had no effect in the as cast structures optimization, since the hardness was not affected.

The parameters for the sintering process must be studied and improved in order to obtain higher densities and homogeneous microstructures, aiming the production of nuclear core parts in near net shape by the powder metallurgy process.

ACKNOWLEDGMENTS

The authors would like to acknowledge to CNPq financial support (contracts nº 306530/2010-4 and 483686/2010-7), to Indústrias Nucleares Brasileiras - INB for providing the Zircaloy chips, to Dr. C. S. Mucsi for helping in furnace operation, to J. H. Duvaizem for helping in sintering and Comissão Nacional de Energia Nuclear - CNEN for a Ph.D. scholarship of L. A. T. Pereira.

REFERENCES

1. A.E. Bohe, J.J. Andrade Gamboa, E.M. Lopasso, D.M. Pasquevich, "Zirconium recovery from Zircaloy shavings", *J. Mater. Sci.* **31**, pp.3469-3474(1996).
2. P. Mukherjee, P. Barat, S.K. Bandyopadhyay, P. Sen, S.K. Chattopadhyay, S.K.C. Jee, A.K. Meikap, M.K. Mitra, "Microstructural studies on lattice imperfections in deformed zirconium-base alloys by X-ray diffraction", *Metallurgical and Materials Transactions* A, **31**, pp.2405-2410 (2010).
3. M. Steinbrück. "Hydrogen absorption by zirconium alloys at high temperatures", *Journal of Nuclear Materials*, **334**, pp.58-64(2004).
4. J.H. Schemel, *Manual on Zirconium and Hafnium, ASTM Special Technical Publication* pp.639 -, (1997).
5. K. Natesan, W.K. Soppet, " Hydrogen Effects on Air Oxidation of Zirlo Alloy" *NUREG/CR–6851*, **ANL-04/14**, Argonne National Laboratory (USA), (2004).
6. Y. Kim, D.R. Olander, "Internal hydriding of defected Zircaloy cladding fuel rods: a review", *Journal of Korean Nuclear Society* **V. 25**, Number 4, (1993).
7. R.W. Dayton, C.M. Allen, W.U. Eberts, "The Reclamation of Zirconium Machining Chips to Produce Arc-Melting Feed Stock*", United States Atomic Energy Commission* **AECD-3499**, (1952).
8. L.A.T. Pereira; C.S. Mucsi, H.P.S. Corrêa, M.T.D. Orlando, I.M. Sato, J.L. Rossi, L.G. Martinez, "Zircaloy chips remelting using VAR: preliminary results", *19º CBECiMat - Congresso Brasileiro de Engenharia e Ciência dos Materiais*, Campos de Jordão - SP, (2010).
9. K. Mimura, S.W. Lee, M. Isshiki, "Removal of alloying elements from zirconium alloys by hydrogen plasma-arc melting", *Journal of Alloys and Compounds*, **221**, pp.267-273 (1995).
10. B. Lustman, F. Kerze Jr.,"*The Metallurgy of Zirconium"* National Nuclear Energy Series, Div. 7, V. 4. McGraw-Hill, New York, (1955).
11. I. Costa, "*Study of the oxidation behavior of zirconium and its alloys"*, Master Dissertation, IPEN/USP, (In Portuguese), São Paulo, (1985).
12. S.N. Doi "*Phase transformation of Zr-Nb alloys",* Master Dissertation, IPEN/USP, (In Portuguese), São Paulo, (1980).
13. Y.H. Jeong, U.C. Kim, "Correlation of cold work, annealing, and microstructure in Zircaloy-4 cladding material", *Journal of the Korean Nuclear Society*, **V.18**, Number 4, (1986).
14. S. Okaguchi, H. Ohtani, Y. Ohmori, "Morphology of Widmanstätten and bainitic ferrites", *Materials Transactions*, JIM, **32/8**, pp. 697-704 (1991).
15. I.M. Sato, L.A.T. Pereira, M.A. Scapin, M.B. Cotrim, C.S. Mucsi, J.L. Rossi, L.G. Martinez, "Chemical and microstructural characterization of remelted Zircaloy by X-ray fluorescence techniques and metallographic analysis", *Journal of Radioanalytical and Nuclear Chemistry* (in print 2011).